# Color flux-tube nature of the states $T_{cs}(2900)$ and $T_{c\bar{s}}^a(2900)$

Jia Wei, Yi-Heng Wang, Chun-Sheng An,\* and Cheng-Rong Deng<sup>†</sup> School of Physical Science and Technology, Southwest University, Chongqing 400715, China

(Received 10 October 2022; accepted 1 November 2022; published 28 November 2022)

DOI: 10.1103/PhysRevD.106.096023

### I. INTRODUCTION

In 2020, the LHCb Collaboration observed two exotic structures with open quark flavors in the invariant mass distribution of  $D^-K^+$  of the channel  $B^+ \to D^+D^-K^+$ , which were denoted as  $X_0(2900)$  and  $X_1(2900)$  [1]. Their masses and widths in MeV are

$$X_0(2900)$$
:  $M = 2866 \pm 7 \pm 2$ ,  $\Gamma = 57 \pm 12 \pm 4$ ,  $X_1(2900)$ :  $M = 2904 \pm 5 \pm 1$ ,  $\Gamma = 110 \pm 11 \pm 4$ .

Both of them have the minimal quark content  $cs\bar{u}\,\bar{d}$  because they can strongly decay into  $D^-K^+$ . The assignments of their spin-parity are  $0^+$  and  $1^-$ , respectively. However, the accurate information on their isospin has not been available until now. Recently, the LHCb Collaboration suggested to rename the states  $X_0(2900)$  and  $X_1(2900)$  as  $T_{cs0}(2900)^0$  and  $T_{cs1}(2900)^0$ , respectively [2].

In 2022, the LHCb Collaboration reported two isospin vector resonances  $T^a_{c\bar{s}0}(2900)^0$  and  $T^a_{c\bar{s}0}(2900)^{++}$  in the  $D^+_s\pi^\pm$  invariant spectrum of the similar channels

Published by the American Physical Society under the terms of the Creative Commons Attribution 4.0 International license. Further distribution of this work must maintain attribution to the author(s) and the published article's title, journal citation, and DOI. Funded by SCOAP<sup>3</sup>.  $B^+ \to \bar{D}^- D_s^+ \pi^+$  and  $B^0 \to \bar{D}^0 D_s^+ \pi^-$  [3]. Their masses and widths are

$$T^a_{c\bar{s}}(2900)^0$$
:  $M = 2892 \pm 21 \pm 2$ ,  $\Gamma = 119 \pm 29$ ,  $T^a_{c\bar{s}}(2900)^{++}$ :  $M = 2921 \pm 23 \pm 2$ ,  $\Gamma = 137 \pm 35$ .

Supposing the states belong to the same isospin triplet, the experiment also gave the shared mass and width,

$$M = 2908 \pm 23 \text{ MeV}, \qquad \Gamma = 136 \pm 25 \text{ MeV}.$$

Their least quark contents are, respectively,  $cd\bar{s} \bar{u}$  and  $cu\bar{s} \bar{d}$  with the same spin-parity  $0^+$ .

The investigation on the structure and property of the states could help us to improve our knowledge of the low-energy strong interaction. Several possible physical pictures, molecular states  $\bar{D}^*K^*$ ,  $\bar{D}_1K$ , and  $D_s^*\rho$  [4–17], compact state  $[cs][\bar{u}\bar{d}]$  [18–28], tetramole (superposition of molecules and compact tetraquark states) [29], triangle singularity [30,31], and kinematical cusp [32] were proposed within various theoretical frameworks. Most of the interpretations on the states  $T_{cs0}(2900)^0$  and  $T_{cs1}(2900)^0$  preferred an isospin singlet. Especially for the molecular states, the channel can produce a little attraction by meson exchange interaction, which is beneficial to form bound states. We refer interested readers to the latest reviews for more comprehensive descriptions [33].

In the present work, we prepare to make a systematical investigation of the ground and first angular excited states

ancs@swu.edu.cn crdeng@swu.edu.cn

 $[cs][\bar{u}\ \bar{d}]$  and  $[cu][\bar{s}\ \bar{d}]$  with all possible spin, isospin, and color combinations in the multiquark color flux-tube model (MCFTM). We anticipate broadening the property and structure of the four states from the perspective of the diquark picture and providing some valuable clues to the experimental establishment of the tetraquark states in the future. We also hope that this work can improve the understanding of the mechanism of the low-energy strong interaction.

This paper is organized as follows. After the Introduction section, we give a concise description of the MCFTM in Sec. II. We introduce the trial wave functions of the states  $[cs][\bar{u}\ \bar{d}]$  in Sec. III. We present the numerical results and discussions in Sec. IV. We list a brief summary in the last section.

### II. MULTIQUARK COLOR FLUX-TUBE MODEL

The MCFTM [34] has been established on the basis of the color flux-tube picture in lattice QCD [35,36] and the chiral constituent quark model [37]. We only give the schemata of the model here. The model Hamiltonian reads

$$H_{n} = \sum_{i=1}^{n} \left( m_{i} + \frac{\mathbf{p}_{i}^{2}}{2m_{i}} \right) - T_{c} + V^{\text{CON}}(n) + \sum_{i>j}^{n} V_{ij},$$

$$V_{ij} = V_{ij}^{\text{OGE}} + V_{ij}^{\text{OBE}} + V_{ij}^{\sigma}, \tag{1}$$

where  $m_i$  and  $\mathbf{p}_i$  are the mass and momentum of the ith quark or antiquark, respectively.  $T_c$  is the center-of-mass kinetic energy of the states and should be deducted.  $V^{\text{CON}}(n)$  is an n-body color confinement potential.  $V^{\text{OGE}}_{ij}$ ,  $V^{\text{OBE}}_{ij}$ , and  $V^{\sigma}_{ij}$  are the one-gluon-exchange interaction, the one-boson-exchange interaction between the particles i and j, respectively. In the state  $[cs][\bar{u}\,\bar{d}]$ , the codes of c, s,  $\bar{u}$ , and  $\bar{d}$  are assumed to be 1, 2, 3, and 4, respectively. Their corresponding positions are denoted as  $\mathbf{r}_1$ ,  $\mathbf{r}_2$ ,  $\mathbf{r}_3$ , and  $\mathbf{r}_4$ . The codes of the state  $[cu][\bar{s}\,\bar{d}]$  are exactly the same as those of the state  $[cs][\bar{u}\,\bar{d}]$ .

For mesons, the quark and antiquark are linked by a three-dimensional color flux tube. Its two-body square confinement potential reads

$$V^{\text{CON}}(2) = kr_{a\bar{a}}^2, \tag{2}$$

where  $r_{q\bar{q}}$  is the distance between q and  $\bar{q}$ , and k is the stiffnesses of a three-dimensional color flux tube determined by fitting the meson spectrum.

Within the framework of the diquark-antidiquark configuration, the states  $[cs][\bar{u}\ \bar{d}]$  and  $[cu][\bar{s}\ \bar{d}]$  have a double-Y-type color flux-tube structure. Its four-body confinement potential reads

$$V^{\text{CON}}(4) = k((\mathbf{r}_1 - \mathbf{y}_{12})^2 + (\mathbf{r}_2 - \mathbf{y}_{12})^2 + (\mathbf{r}_3 - \mathbf{y}_{34})^2 + (\mathbf{r}_4 - \mathbf{y}_{34})^2 + \kappa_d(\mathbf{y}_{12} - \mathbf{y}_{34})^2), \tag{3}$$

where  $\mathbf{y}_{12}$  and  $\mathbf{y}_{34}$  stand for the positions of the two Y-shaped junctions. In order to satisfy the requirement of the overall color singlet, the color flux tube connecting  $\mathbf{y}_{12}$  and  $\mathbf{y}_{34}$  must be given by the SU(3) color representations  $\mathbf{\bar{3}}_c$  or  $\mathbf{6}_c$ . The relative stiffness parameter  $\kappa_d$  of the d-dimensional color flux tube is equal to  $\frac{C_d}{C_3}$  [38–40], where  $C_d$  is the eigenvalue of the Casimir operator associated with the SU(3) color representation d at either end of the color flux tube.

Taking  $y_{12}$  and  $y_{34}$  as variational parameters, we determine them by minimizing the four-body confinement potential. With their values, we can obtain the minimum of the confinement potential. Finally, we simplify the minimum into three independent harmonic oscillators

$$V^{\text{CON}}(4) = k \left( \mathbf{R}_1^2 + \mathbf{R}_2^2 + \frac{\kappa_d}{1 + \kappa_d} \mathbf{R}_3^2 \right)$$
 (4)

by diagonalizing the confinement potential matrix.  $\mathbf{R}_i$  are the normal modes of the confinement potential and read

$$\mathbf{R}_{1} = \frac{1}{\sqrt{2}}(\mathbf{r}_{1} - \mathbf{r}_{2}), \qquad \mathbf{R}_{2} = \frac{1}{\sqrt{2}}(\mathbf{r}_{3} - \mathbf{r}_{4}),$$

$$\mathbf{R}_{3} = \frac{1}{\sqrt{4}}(\mathbf{r}_{1} + \mathbf{r}_{2} - \mathbf{r}_{3} - \mathbf{r}_{4}),$$

$$\mathbf{R}_{4} = \frac{1}{\sqrt{4}}(\mathbf{r}_{1} + \mathbf{r}_{2} + \mathbf{r}_{3} + \mathbf{r}_{4}).$$
(5)

One expects the model dynamics to be governed by QCD. The perturbative effect is the well-known one-gluon-exchange (OGE) interaction. From the nonrelativistic reduction of the OGE diagram in QCD for pointlike quarks, one gets

$$V_{ij}^{\text{OGE}} = \frac{\alpha_s}{4} \lambda_i^c \cdot \lambda_j^c \left( \frac{1}{r_{ij}} - \frac{2\pi \delta(\mathbf{r}_{ij}) \boldsymbol{\sigma}_i \cdot \boldsymbol{\sigma}_j}{3m_i m_j} \right), \tag{6}$$

where  $\lambda_i^c$  and  $\sigma_i$  stand for the color SU(3) Gell-Mann matrices and spin SU(2) Pauli matrices, respectively.  $r_{ij}$  is the distance between the particles i and j. The Dirac  $\delta(\mathbf{r}_{ij})$  function should be regularized in the form [37]

$$\delta(\mathbf{r}_{ij}) \to \frac{1}{4\pi r_{ij} r_0^2(\mu_{ij})} e^{-\frac{r_{ij}}{r_0(\mu_{ij})}},$$
 (7)

where  $r_0(\mu_{ij}) = \frac{\hat{r}_0}{\mu_{ij}}$ , and  $\mu_{ij}$  is the reduced mass of two interacting particles i and j. The quark-gluon coupling constant  $\alpha_s$  adopts an effective scale-dependent form given as

$$\alpha_s(\mu_{ij}^2) = \frac{\alpha_0}{\ln\frac{\mu_{ij}^2}{\Lambda_c^2}},\tag{8}$$

where  $\hat{r}_0$ ,  $\Lambda_0$ , and  $\alpha_0$  are adjustable parameters fixed by fitting the ground state meson spectrum.

The origin of the constituent quark mass can be traced back to the spontaneous breaking of  $SU(3)_L \otimes SU(3)_R$ 

chiral symmetry [41]. The chiral symmetry is spontaneously broken in the light sector (u, d, and s) while it is explicitly broken in the heavy sector (c and b). The meson-exchange interactions only occur in the light quark sector. The central parts of the interactions can be resumed as follows [37]:

$$V_{ij}^{OBE} = V_{ij}^{\pi} \sum_{k=1}^{3} \mathbf{F}_{i}^{k} \mathbf{F}_{j}^{k} + V_{ij}^{K} \sum_{k=4}^{7} \mathbf{F}_{i}^{k} \mathbf{F}_{j}^{k} + V_{ij}^{\eta} (\mathbf{F}_{i}^{8} \mathbf{F}_{j}^{8} \cos \theta_{P} - \sin \theta_{P}),$$

$$V_{ij}^{\chi} = \frac{g_{ch}^{2}}{4\pi} \frac{m_{\chi}^{3}}{12m_{i}m_{j}} \frac{\Lambda_{\chi}^{2}}{\Lambda_{\chi}^{2} - m_{\chi}^{2}} \sigma_{i} \cdot \sigma_{j} \left( Y(m_{\chi}r_{ij}) - \frac{\Lambda_{\chi}^{3}}{m_{\chi}^{3}} Y(\Lambda_{\chi}r_{ij}) \right), \qquad Y(x) = \frac{e^{-x}}{x},$$

$$V_{ij}^{\sigma} = -\frac{g_{ch}^{2}}{4\pi} \frac{\Lambda_{\sigma}^{2} m_{\sigma}}{\Lambda_{\sigma}^{2} - m_{\sigma}^{2}} \left( Y(m_{\sigma}r_{ij}) - \frac{\Lambda_{\sigma}}{m_{\sigma}} Y(\Lambda_{\sigma}r_{ij}) \right). \tag{9}$$

 $F_i$  are the flavor SU(3) Gell-Mann matrices and  $\chi$  represents  $\pi$ , K, and  $\eta$ . The mass parameters  $m_{\chi}$  take their experimental values, while the cutoff parameters  $\Lambda_{\chi}$  and the mixing angles  $\theta_P$  take the values from [37]. The mass parameter  $m_{\sigma}$  can be determined through the partially conserved axial vector current relation  $m_{\sigma}^2 \approx m_{\pi}^2 + 4m_{u,d}^2$  [42]. The chiral coupling constant  $g_{ch}$  can be obtained from the  $\pi NN$  coupling constant through

$$\frac{g_{ch}^2}{4\pi} = \left(\frac{3}{5}\right)^2 \frac{g_{\pi NN}^2}{4\pi} \frac{m_{u,d}^2}{m_N^2}.$$
 (10)

The most prominent characteristic is the application of the multibody confinement potential based on the color flux-tube picture instead of the two-body one in the other quark models.

#### III. WAVE FUNCTIONS

Within the framework of the diquark-antidiquark configuration, the trial wave function of the state  $[cs][\bar{u}\ \bar{d}]$  with  $I(J^P)$  can be constructed as a sum of the following direct products of color  $\varphi_c$ , isospin  $\varphi_i$ , spin  $\varphi_s$ , and spatial  $\phi$  terms,

$$\Phi_{IJ}^{[cs][\bar{u}\,\bar{d}]} = \sum_{\alpha} c_{\alpha} [[[\phi_{l_{a}m_{a}}(\mathbf{r}_{a})\varphi_{s_{a}}]_{J_{a}}[\phi_{l_{b}m_{b}}(\mathbf{r}_{b})\varphi_{s_{b}}]_{J_{b}}]_{J_{ab}} 
\times \phi_{l_{c}m_{c}}(\mathbf{r}_{c})]_{JM_{J}}^{[cs][\bar{u}\,\bar{d}]} [\varphi_{i_{a}}\varphi_{i_{b}}]_{IM_{I}}^{[cs][\bar{u}\,\bar{d}]} [\varphi_{c_{a}}\varphi_{c_{b}}]_{\mathbf{1}_{c}}^{[cs][\bar{u}\,\bar{d}]}.$$
(11)

The subscripts a and b represent the diquark [cs] and antidiquark  $[\bar{u}\ \bar{d}]$ , respectively. The square brackets imply all possible Clebsch-Gordan couplings. The summation

index  $\alpha$  represents all of possible channels and the coefficient  $c_{\alpha}$  is determined by the model dynamics.

In order to obtain reliable numerical results, the precision numerical method is indispensable. The Gaussian expansion method [43], which has been proven to be rather powerful to solve the few-body problem, is therefore used in the present work. According to the Gaussian expansion method, the relative motion wave function can be written as

$$\phi_{lm}^{G}(\mathbf{x}) = \sum_{n=1}^{n_{\text{max}}} c_n N_{nl} x^l e^{-\nu_n x^2} Y_{lm}(\hat{\mathbf{x}}), \tag{12}$$

where **x** represents the Jacobian coordinates  $\mathbf{r}_a$ ,  $\mathbf{r}_b$ , and  $\mathbf{r}_c$ ,

$$\mathbf{r}_{a} = \mathbf{r}_{1} - \mathbf{r}_{2}, \qquad \mathbf{r}_{b} = \mathbf{r}_{3} - \mathbf{r}_{4},$$

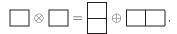
$$\mathbf{r}_{c} = \frac{m_{1}\mathbf{r}_{1} + m_{2}\mathbf{r}_{2}}{m_{1} + m_{2}} - \frac{m_{3}\mathbf{r}_{3} + m_{4}\mathbf{r}_{4}}{m_{3} + m_{4}}, \qquad (13)$$

to describe the relative motions in the state  $[cs][\bar{u}\,\bar{d}]$ . The corresponding angular excitations of three relative motions are, respectively,  $l_a$ ,  $l_b$ , and  $l_c$ . In this work, we assume that the angular excitation only occurs between the diquark [cs] and the antidiquark  $[\bar{u}\,\bar{d}]$  so that the P parity of the state is  $(-1)^{l_c}$ . The Gaussian size  $\nu_n$  is taken as geometric progression

$$\nu_n = \frac{1}{r_n^2}, \qquad r_n = r_1 d^{n-1}, \qquad d = \left(\frac{r_{\text{max}}}{r_1}\right)^{\frac{1}{n_{\text{max}}-1}}, \tag{14}$$

where  $r_1$  and  $r_{\rm max}$  are the minimum and maximum of the size, respectively.  $n_{\rm max}$  is the number of the Gaussian wave function. More details about the Gaussian expansion method can be found in Ref. [43]. In the present work, we can obtain the convergent results by taking  $n_{\rm max}=7$ ,  $r_1=0.1$  fm, and  $r_{\rm max}=2.0$  fm.

The quark is in  $\mathbf{3}_c$  and the antiquark is in  $\mathbf{\bar{3}}_c$ . The color representation of the diquark  $[cs]_{c_a}$  is antisymmetric  $\mathbf{\bar{3}}_c$  or symmetric  $\mathbf{6}_c$ ,



The color representation of the antidiquark  $[\bar{u} \ \bar{d}]_{c_b}$  is antisymmetric  $\mathbf{\bar{6}}_c$ ,

According to the requirement of the overall color singlet of the state  $[cs][\bar{u}\,\bar{d}]$ , there are two ways of coupling the diquark  $[cs]_{c_a}$  and antidiquark  $[\bar{u}\,\bar{d}]_{c_b}$  into an overall color singlet:  $[[cs]_{\bar{3}_c}[\bar{u}\,\bar{d}]_{\bar{3}_c}]_1$  and  $[[cs]_{\bar{6}_c}[\bar{u}\,\bar{d}]_{\bar{6}_c}]_1$ ,

$$\begin{split} \left[ [cs]_{\mathbf{\bar{3}}_c} [\bar{u}\bar{d}]_{\mathbf{\bar{3}}_c} \right]_{\mathbf{1}} = & \frac{1}{\sqrt{3}} \left( \begin{bmatrix} \mathbf{r} & \mathbf{r} & \mathbf{b} \\ \mathbf{g} & \mathbf{b} \end{bmatrix} + \begin{bmatrix} \mathbf{r} & \mathbf{r} & \mathbf{r} \\ \mathbf{g} & \mathbf{b} \end{bmatrix} + \begin{bmatrix} \mathbf{r} & \mathbf{g} \\ \mathbf{g} & \mathbf{b} \end{bmatrix} + \begin{bmatrix} \mathbf{r} & \mathbf{g} \\ \mathbf{g} & \mathbf{b} \end{bmatrix} \right), \\ \left[ [cs]_{\mathbf{6}_c} [\bar{u}\bar{d}]_{\mathbf{\bar{6}}_c} \right]_{\mathbf{1}} = & \frac{1}{\sqrt{6}} \left( \begin{bmatrix} \mathbf{r} & \mathbf{g} & \mathbf{g} & \mathbf{g} \\ \mathbf{b} & \mathbf{b} \end{bmatrix} + \begin{bmatrix} \mathbf{g} & \mathbf{g} \\ \mathbf{g} & \mathbf{b} \end{bmatrix} + \begin{bmatrix} \mathbf{r} & \mathbf{r} \\ \mathbf{g} & \mathbf{b} \end{bmatrix} + \begin{bmatrix} \mathbf{r} & \mathbf{r} \\ \mathbf{g} & \mathbf{g} \end{bmatrix} \right) \\ + \begin{bmatrix} \mathbf{r} & \mathbf{r} \\ \mathbf{g} & \mathbf{g} \end{bmatrix} + \begin{bmatrix} \mathbf{g} & \mathbf{g} \\ \mathbf{g} & \mathbf{g} \end{bmatrix} + \begin{bmatrix} \mathbf{g} & \mathbf{g} \\ \mathbf{g} & \mathbf{g} \end{bmatrix} \right). \end{split}$$

The diquark  $[cs]_{s_a}$  and antidiquark  $[\bar{u}\ \bar{d}]_{s_b}$  can be in the spin singlet or triplet,

The total spin S of the state  $[[cs]_{s_a}[\bar{u}\ \bar{d}]_{s_b}]_S$  can be expressed as  $S=s_a\oplus s_b$ , and its value could be 0, 1, or 2. For the state with S=0, it has two coupling modes,  $0=0\oplus 0$  and  $1\oplus 1$ . Their spin wave function reads

$$\begin{split} \left[ [cs]_0 \oplus \left[ \bar{u} \bar{d} \right]_0 \right]_0 &= \left[ \begin{matrix} \uparrow \\ \downarrow \end{matrix} \right]_{\downarrow} \\ \\ \left[ [cs]_1 \oplus \left[ \bar{u} \bar{d} \right]_1 \right]_0 &= \frac{1}{\sqrt{3}} \left( \begin{matrix} \uparrow \uparrow \uparrow \downarrow \downarrow \downarrow \end{matrix} - \begin{matrix} \uparrow \uparrow \uparrow \uparrow \downarrow \downarrow \downarrow \end{matrix} \right) \\ &+ \left[ \begin{matrix} \downarrow \downarrow \downarrow \downarrow \uparrow \uparrow \uparrow \end{matrix} \right), \end{split}$$

where  $\uparrow$  and  $\downarrow$  stand for spin-up and spin-down, respectively. For the state with S=1, it has three coupling modes,  $0\oplus 1$ ,  $1\oplus 0$ , and  $1\oplus 1$ . Assuming the magnetic component  $M_s=S$ , the corresponding spin wave function reads

$$\begin{split} & \left[ [cs]_0 \oplus \left[ \bar{u} \bar{d} \right]_1 \right]_1 = \overline{\bigoplus} \, \uparrow \uparrow \uparrow \, , \\ & \left[ [cs]_1 \oplus \left[ \bar{u} \bar{d} \right]_0 \right]_1 = \overline{\uparrow} \uparrow \uparrow \uparrow \downarrow \, , \\ & \left[ [cs]_1 \oplus \left[ \bar{u} \bar{d} \right]_1 \right]_1 = \frac{1}{\sqrt{2}} \left( \uparrow \uparrow \uparrow \uparrow \downarrow - \uparrow \downarrow \uparrow \uparrow \uparrow \right) \, . \end{split}$$

For the state with S = 2, its spin wave function reads

$$\left[ [cs]_1 \oplus [\bar{u}\bar{d}]_1 \right]_2 = \boxed{\uparrow} \boxed{\uparrow} \boxed{\uparrow}.$$

The total isospin of the state is only determined by the antidiquark  $[\bar{u} \, \bar{d}]_{i_b}$  because of the zero isospin of the diquark  $[cs]_{i_a}$ . Like the spin of the diquark or antidiquark, the antidiquark  $[\bar{u} \, \bar{d}]_{i_b}$  can be an isospin singlet and triplet. The isospin wave function reads

$$\left[ [cs]_0 [\bar{u}\bar{d}]_0 \right]_0 = cs \left[ \overline{\underline{u}} \right], \quad \left[ [cs]_0 [\bar{u}\bar{d}]_1 \right]_1 = cs \left[ \overline{\underline{u}} | \overline{d} \right].$$

The diquark and antidiquark are a spatially extended compound with various color-flavor-spin-space configurations [44]. The substructure of the diquarks may affect the structure of the multiquark states. Taking all degrees of freedom of identical quarks  $\bar{u}$  and  $\bar{d}$  into account, the Pauli principle imposes some restrictions on the antidiquark  $[\bar{u}\ \bar{d}]$ .  $i_b + s_b =$  even if the antidiquark is in  $\mathbf{3}_c$ , while  $i_b + s_b =$  odd if the antidiquark is in  $\bar{\mathbf{6}}_c$ .

The corresponding SU(2) groups of the isospin and the so-called V spin and U spin are three subgroups of the flavor SU(3) group. The U spin of the antidiquark  $[\bar{s}\ \bar{d}]$ , the V spin of the antidiquark  $[\bar{s}\ \bar{u}]$ , and the isospin of the antidiquark  $[\bar{u}\ \bar{d}]$  have similar symmetry in their flavor wave functions. Therefore, the total wave functions of the states  $[cs][\bar{u}\ \bar{d}]$ ,  $[cu][\bar{s}\ \bar{d}]$ , and  $[cd][\bar{s}\ \bar{u}]$  have exactly the same structure if the flavor SU(3) symmetry is involved. In order to avoid valueless repetition, we just present the details of the wave function construction for the state  $[cs][\bar{u}\ \bar{d}]$ .

## IV. NUMERICAL RESULTS AND ANALYSIS

### A. Meson spectrum and adjustable model parameters

We can determine the adjustable model parameters by solving the two-body Schrödinger equation to fit the ground state meson spectrum in the MCFTM. With the

TABLE I. Adjustable model parameters, quark mass, and  $\Lambda_0$  unit in MeV, k unit in MeV · fm<sup>-2</sup>,  $r_0$  unit in MeV · fm, and  $\alpha_0$  is dimensionless.

Parameter	$m_{u,d}$	$m_s$	$m_c$	k	$\alpha_0$	$\Lambda_0$	$r_0$
Value	280	488	1653	458	3.99	30.34	65.15

TABLE II. Ground state meson spectrum, units in MeV.

State	π	ρ	ω	K	<i>K</i> *	φ	$D^{\pm}$
Theory Particle data group						1047 1020	
States	$D^*$	$D_s^\pm$	$D_s^*$	$\eta_c$	$J/\Psi$		
Theory Particle data group			2146 2112				

MINUIT program [45], we can obtain a set of optimal parameters and the meson spectrum, which are presented in Tables I and II, respectively.

## B. $[cs][\bar{u}\ \bar{d}]$ spectrum and candidates of $T_{cs}(2900)$

In the following, we concentrate on the properties of the ground and *P*-wave states  $[cs][\bar{u}\ \bar{d}]$  with various spin,

isospin, and color combinations in the MCFTM with the parameters determined by the meson spectrum. Note that we do not introduce any new adjustable parameters in the calculation of the tetraquark states.

Solving the four-body Schrödinger equation with the well-defined trial wave function, we can obtain the eigenenergies of the states  $[cs][\bar{u}\,\bar{d}]$ , which are presented in Table III.  $\bar{\bf 3}_c$ - ${\bf 3}_c$  and  ${\bf 6}_c$ - $\bar{\bf 6}_c$ , respectively, stand for the state  $[cs][\bar{u}\,\bar{d}]$  with the color configurations  $[[cs]_{\bar{\bf 3}_c}[\bar{u}\,\bar{d}]_{\bar{\bf 3}_c}]_1$  and  $[[cs]_{\bar{\bf 6}_c}[\bar{u}\,\bar{d}]_{\bar{\bf 6}_c}]_1$ . C.C. represents the coupling of the two color configurations. We calculate the ratio of each color configuration in the coupled channels using the corresponding eigenvectors. In addition, we calculate the contribution coming from each part of the Hamiltonian in each color configuration and the coupled channels, which are presented in each row in Table III.

In order to illustrate the spatial configuration of the states, we also calculate the average distance between two

TABLE III. Mass of the state  $[cs][\bar{u}\ \bar{d}]$  and contribution from each part of the Hamiltonian unit in MeV and the average distance units in fm,  $J = l_c \oplus S$ .  $\bar{\bf 3}_c - {\bf 3}_c$  and  ${\bf 6}_c - \bar{\bf 6}_c$  stand for the states  $[cs][\bar{u}\ \bar{d}]$  with the color configurations  $[[cs]_{\bar{\bf 3}_c}[\bar{u}\ \bar{d}]_{{\bf 3}_c}]_{\bf 1}$  and  $[[cs]_{\bar{\bf 6}_c}[\bar{u}\ \bar{d}]_{\bar{\bf 6}_c}]_{\bf 1}$ , respectively. C.C. represents the coupling of the two color configurations.  $E_k$ ,  $V^{\rm CON}$ ,  $V^{\rm CM}$ ,  $V^{\rm C}$ ,  $V^{\eta}$ ,  $V^{\kappa}$ , and  $V^{\kappa}$  represent kinetic energy, confinement potential, color-magnetic interaction, Coulomb interaction,  $\eta$ -,  $\pi$ -, K-, and  $\sigma$ -exchange interactions, respectively.

$l_c$	S	$IJ^P$	Color	Mass, Ratio	$\langle E_k \rangle$	$\langle V^{\rm CON} \rangle$	$\langle V^{\mathrm{CM}} \rangle$	$\langle V^{\rm C} \rangle$	$\langle V^\eta  angle$	$\langle V^\pi \rangle$	$\langle V^K \rangle$	$\langle V^{\sigma} \rangle$	$\langle \mathbf{r}_{12}^2 \rangle^{\frac{1}{2}}$	$\langle \mathbf{r}_{34}^2 \rangle^{\frac{1}{2}}$	$\langle \mathbf{r}_{13}^2 \rangle^{\frac{1}{2}}$	$\langle \mathbf{r}_{24}^2 \rangle^{\frac{1}{2}}$	$\langle {f r}_c^2  angle^{1\over 2}$
			$\bar{3}_c$ - $3_c$	2559, 84%	1491	275	-284	-1201	72	-401	0	-94	0.63	0.66	0.71	0.85	0.61
	0	$00^{+}$	$6_c$ - $\mathbf{\bar{6}}_c$	2830, 16%	1099	340	-211	-1066	2	38	0	-73	0.67	0.89	0.68	0.85	0.50
			C.C.	2495	1571	255	-409	-1248	63	-339	0	<b>-</b> 99	0.60	0.67	0.66	0.80	0.56
			$\bar{3}_c$ - $3_c$	2604, 98%	1430	290	-235	-1164	72	-399	0	<b>-</b> 91	0.67	0.66	0.72	0.87	0.62
0	1	$01^{+}$	$6_c$ - $\bar{6}_c$	3008, 2%	907	402	-5	-962	-3	30	0	-62	0.74	0.95	0.75	0.93	0.55
			C.C.	2591	1444	285	-255	-1173	70	-389	0	-92	0.66	0.66	0.71	0.86	0.61
	2	$02^{+}$	$6_c$ - $\bar{6}_c$	3068, 100%	852	423	55	-926	<b>-</b> 5	27	0	<b>–</b> 59	0.76	0.97	0.77	0.95	0.57
			$\bar{3}_c$ - $3_c$	2940, 78%	955	366	-12	-984	-2	-16	0	-68	0.67	0.88	0.78	0.92	0.62
	0	$10^{+}$	$6_c$ - $\mathbf{\bar{6}}_c$	3068, 22%	860	430	42	-935	5	22	0	-57	0.75	1.00	0.78	0.95	0.56
			C.C.	2871	1036	346	-107	-1028	1	-6	0	-72	0.65	0.87	0.73	0.88	0.59
			$\bar{3}_c$ - $3_c$	2949, 84%	955	370	1	-989	-6	-16	0	-67	0.64	0.89	0.80	0.93	0.64
0	1	$11^{+}$	$6_c$ - $\bar{6}_c$	3056, 16%	870	424	31	-939	5	22	0	-58	0.74	1.00	0.77	0.94	0.59
			C.C.	2979	989	362	-44	-1007	<b>-</b> 4	<b>-</b> 9	0	<b>-</b> 9	0.64	0.89	0.77	0.90	0.61
	2	12+	$\bar{3}_c$ - $3_c$	3018, 100%	878	395	72	-942	<b>-</b> 8	-15	0	<b>−</b> 63	0.69	0.90	0.82	0.96	0.66
			$\bar{3}_c$ - $3_c$	2901, 98%	1468	391	-267	-1014	67	-375	0	-70	0.67	0.96	1.08	0.97	0.89
	0	01-	$6_c$ - $\mathbf{\bar{6}}_c$	3341, 2%	1007	502	-108	-739	1	24	0	-47	0.77	1.01	0.92	1.09	0.75
			C.C.	2893	1478	385	-283	-1017	66	-367	0	-70	0.66	0.69	0.95	1.07	0.88
			$\bar{3}_c$ - $3_c$	2940, 99%	1421	406	-224	-987	67	-375	0	-69	0.71	0.69	0.97	1.10	0.89
1	1	$00^-, 01^-, 02^-$	$6_c$ - $\bar{6}_c$	3433, 1%	912	545	-5	-697	-2	22	0	<b>-43</b>	0.81	1.04	0.97	1.14	0.80
			C.C.	2938	1424	404	-228	<b>-</b> 987	66	-373	0	-69	0.71	0.69	0.97	1.10	0.90
	2	01-,02-,03-	$6_c$ - $\bar{6}_c$	3464, 100%	882	557	26	<b>-</b> 679	<b>-</b> 3	21	0	<b>-4</b> 1	0.81	1.05	0.99	1.16	0.81
			$\bar{3}_c$ - $3_c$	3275, 94%	967	491	13	-831	-4	-14	0	-48	0.71	0.93	1.01	1.14	0.87
	0	11-	$6_c$ - $\bar{6}_c$	3475, 6%	886	566	33	-690	3	16	0	<b>-4</b> 0	0.82	1.09	0.99	1.16	0.80
			C.C.	3259	990	582	-16	-834	-3	-12	0	<b>-49</b>	0.70	0.93	0.99	1.12	0.86
			$\bar{3}_c$ - $3_c$	3265, 98%	987	489	1	-846	-5	-14	0	-48	0.67	0.93	1.02	1.14	0.90
1	1	10-, 11-, 12-	$6_c$ - $\bar{6}_c$	3471, 2%	892	565	25	<b>-691</b>	3	16	0	<b>-4</b> 0	0.80	1.08	0.98	1.15	0.80
	_		C.C.	3259	994	487	<b>-</b> 9	-847	-5	-13	0	-48	0.67	0.93	1.02	1.13	0.90
_	2	11-, 12-, 13-	$\bar{3}_c$ - $3_c$	3316, 100%	929	510	56	-814	-6	-14	0	-46	0.71	0.93	1.04	1.17	0.92

quarks  $\langle {\bf r}_{ij}^2 \rangle^{\frac{1}{2}}$  and the relative distance  $\langle {\bf r}_c^2 \rangle^{\frac{1}{2}}$  between the diquark [cs] and the antidiquark  $[\bar{u}\,\bar{d}]$ , which are listed in Table III.  $\langle {\bf r}_{12}^2 \rangle^{\frac{1}{2}}$  and  $\langle {\bf r}_{34}^2 \rangle^{\frac{1}{2}}$  represent the size of the diquark [cs] and antidiquark  $[\bar{u}\,\bar{d}]$ , respectively.  $\langle {\bf r}_{13}^2 \rangle^{\frac{1}{2}}$  is equal to  $\langle {\bf r}_{14}^2 \rangle^{\frac{1}{2}}$  and  $\langle {\bf r}_{23}^2 \rangle^{\frac{1}{2}}$  is equal to  $\langle {\bf r}_{24}^2 \rangle^{\frac{1}{2}}$  because the quarks  $\bar{u}$  and  $\bar{d}$  are considered as identical particles. All of the distances are less than or around 1 fm, so that the states  $[cs][\bar{u}\,\bar{d}]$  should be a compact spatial configuration in the model because of the multibody confinement potential, which is a collective degree of freedom and binds all particles together.

For the ground states, the diquark [cs] and the anti-diquark  $[\bar{u}\ \bar{d}]$  have a strong overlap because of the smaller distance  $\langle \mathbf{r}_c^2 \rangle^{\frac{1}{2}}$  relative to the sizes of the diquark [cs] and antidiquark  $[\bar{u}\ \bar{d}]$ , see  $\langle \mathbf{r}_{12}^2 \rangle^{\frac{1}{2}}$ ,  $\langle \mathbf{r}_{34}^2 \rangle^{\frac{1}{2}}$ , and  $\langle \mathbf{r}_c^2 \rangle^{\frac{1}{2}}$ . For the P-wave states, the sizes of the diquark [cs] and antidiquark  $[\bar{u}\ \bar{d}]$  do not change dramatically relative to those of the corresponding ground states because the angular excitation only occurs between the diquark [cs] and antidiquark  $[\bar{u}\ \bar{d}]$ . However, the distance between the diquark [cs] and antidiquark  $[\bar{u}\ \bar{d}]$  obviously increases; also see  $\langle \mathbf{r}_{12}^2 \rangle^{\frac{1}{2}}$ ,  $\langle \mathbf{r}_{34}^2 \rangle^{\frac{1}{2}}$ , and  $\langle \mathbf{r}_c^2 \rangle^{\frac{1}{2}}$ . The P-wave states look like a dumbbell-like spatial configuration because the [cs] and  $[\bar{u}\ \bar{d}]$  are separated gradually.

One can find from Table III that the  $\bar{\bf 3}_c$ - ${\bf 3}_c$  is dominant in the states with S=0 and 1, especially for the states  $[cs][\bar u\,\bar d]$  with I=0. In the  $\bar{\bf 3}_c$ - ${\bf 3}_c$ , the interactions  $V^{\rm CM}$ ,  $V^{\rm C}$ , and  $V^{\pi}$  can give much stronger attractions than they do in the  ${\bf 6}_c$ - $\bar{\bf 6}_c$ . With the increasing of the mass ratio of  $m_Q$  and  $m_{\bar q}$ , where Q=s, c, or b and  $\bar q=\bar u$  or  $\bar d$ , the  $\bar{\bf 3}_c$ - ${\bf 3}_c$  gradually increase in the states  $[QQ][\bar u\,\bar d]$  [46]. The underlying dynamical mechanism of such phenomenological regularity in the  $\bar{\bf 3}_c$ - ${\bf 3}_c$  is governed by the color Coulomb interaction in the diquark [QQ] and the color-magnetic interaction and the  $\pi$ -meson exchange in the antidiquark  $[\bar u\,\bar d]$  [44]. The single color configuration of the high-spin (S=2) states is uniquely determined by the symmetry of their wave functions.

The ground state  $[cs][\bar{u}\,\bar{d}]$  with  $I(J^P)=0(0^+)$  and  $\bar{\bf 3}_c$ - $\bf 3}_c$  has a low mass of 2559 MeV due to the strong  $\pi$ -meson exchange. After coupling with the  $\bf 6}_c$ - $\bar{\bf 6}_c$ , the mass of the state with  $0(0^+)$  is further pushed down to 2495 MeV, which is much lower, about 370 MeV, than that of the state  $T_{cs0}(2900)^0$  reported by the LHCb Collaboration. Therefore, the state  $T_{cs0}(2900)^0$  cannot be seen as the state  $[cs][\bar{u}\,\bar{d}]$  with  $0(0^+)$  in the model. A similar model study on the state  $[cs][\bar{u}\,\bar{d}]$  was carried out in Refs. [24,25], where the authors did not take into account the meson exchange in their models. None of their predicted masses of the state with  $0(0^+)$  can match that of the state  $T_{cs0}(2900)^0$ . In other words, the state  $T_{cs0}(2900)^0$  may be not the compact state  $[cs][\bar{u}\,\bar{d}]$  with  $0(0^+)$  in the quark models with

QCD-inspired dynamics. However, various color-magnetic models without explicit dynamics can interpret the main component of the state  $T_{cs0}(2900)^0$  as the compact state  $[cs][\bar{u}\ \bar{d}]$  with  $0(0^+)$  [21,22]. On the other hand, the color-magnetic models do not seem to completely absorb the dynamic effect by the effective masses of the constituent quarks [47].

The ground state  $[cs][\bar{u}\ \bar{d}]$  with  $I(J^P)=0(0^+)$  is about 100 MeV higher than that of the state with  $0(0^+)$  mainly due to the relative weak color-magnetic interaction and Coulomb interaction. The  $\mathbf{6}_c$ - $\bar{\mathbf{6}}_c$  has a very tiny probability, just 2%, so that it can be abandoned in the state  $[cs][\bar{u}\ \bar{d}]$  with  $0(1^+)$ . The state  $[cs][\bar{u}\ \bar{d}]$  with  $0(2^+)$  has a very high energy of 3068 MeV because of the absence of the  $\bar{\mathbf{3}}_c$ -3 $_c$ .

For the ground states with  $I(J^P)=1(0^+)$  and  $1(1^+)$ , their masses are much higher than the states with  $0(0^+)$  and  $0(1^+)$ , respectively. Such regularity also holds true for their corresponding P-wave states with I=0 and 1, see Table III, which mainly originates from the different contribution of the  $\pi$ -meson exchange. This provides very strong attraction in the states with I=0, while it gives a weak interaction in the states with I=1. For the high-spin (S=2) ground states, the mass splitting between the states with I=0 and I=1 resulting from the  $\pi$ -meson exchange is not as obvious as the low-spin states.

In the ground state  $[cs][\bar{u}\ \bar{d}]$  with  $I(J^P)=1(0^+)$ , its main color configuration is  $\bar{\bf 3}_c$ - ${\bf 3}_c$ , reaching 78%, and its corresponding spin configuration is  $1\oplus 1$ , namely, consisting of an axial vector  $[cs]_{\bar{\bf 3}_c}$  and an axial vector  $[\bar{u}\ \bar{d}]_{{\bf 3}_c}$ , see Table III. Its mass, about 2923 MeV, is slightly higher than that of the state  $T_{cs0}(2900)^0$ . Taking the coupling with the  ${\bf 6}_c$ - $\bar{\bf 6}_c$  into account, the mass can be pushed down to 2871 MeV, which is highly consistent with that of the state  $T_{cs0}(2900)^0$ . In this way, we can describe the state  $T_{cs0}(2900)^0$  as the ground state  $[cs][\bar{u}\ \bar{d}]$  with  $1(0^+)$  in the MCFTM, which is supported by the conclusions of the similar model research and QCD sum rule [24,26]. If the state  $T_{cs0}(2900)^0$  really belongs to an isotriplet, its charged partners would be abundant, which deserves further research in the future.

On the contrary, the diquark picture  $[cs][\bar{u}\,\bar{d}]$  seems to prefer the  $I(J^P)$  assignment of  $O(0^+)$  in the color-magnetic models and QCD sum rule [21–23]. Assuming the state  $T_{cs0}(2900)^0$  is determined to be isosinglet eventually, the molecular configuration  $\bar{D}^*K^*$  may be a suitable candidate in the models. In order to discriminate all possible interpretations, Burns and Swanson carried out an exhaustive analysis on their decay behaviors as well as their productions in  $B^0$  and  $B^+$  decays [32].

In the *P*-wave states, we do not consider the spin-orbit interaction in the present work because its contributions are very small, just about several MeV [34]. It does not change the qualitative conclusions for the compact tetraquark

states. The spin singlet with  $0(1^-)$  has a mass of 2893 MeV in the MCFTM, see Table III, which is in good agreement with that of the state  $T_{cs1}(2900)^0$ . Its dominant component is composed of a scalar  $[cs]_{\bar{3}_c}$  and a scalar  $[\bar{u} \, \bar{d}]_{\bar{3}_c}$ . In addition, the spin triplet with  $O(1^-)$  has a mass of about 2938 MeV and it consists of a scalar  $[\bar{u} d]_3$  and an axial vector  $[cs]_{\bar{3}}$ . The state is not far away from the state  $T_{cs1}(2900)^0$  so that we cannot rule out the fact that its main component may be made of a scalar  $[\bar{u} \, \bar{d}]_{3}$  and an axial vector  $[cs]_{\bar{3}}$ . In other words, we can describe the state  $T_{cs1}(2900)^0$  as the compact state  $[\bar{u}\ \bar{d}]_{3_c}$  with  $0(1^-)$  in the MCFTM. Its main component could consist of a scalar or an axial vector  $[cs]_{\bar{3}_c}$  and a scalar  $[\bar{u} \, \bar{d}]_{\bar{3}_c}$ . Whichever description in the compact state  $[cs][\bar{u}\ \bar{d}]$  and molecular state  $D_1 K$ , the state  $T_{cs1}(2900)^0$  seems to prefer the  $I(J^P)$ assignment of  $0(1^-)$  [13–15,18,20].

The states with  $0(1^-)$  and S = 2 are much higher, about 500 MeV, than the state  $T_{cs1}(2900)^0$ , which should not be

the main component of the state  $T_{cs1}(2900)^0$ . All of the P-wave states with I=1 have similar masses, around 3300 MeV, which are also much higher than the state  $T_{cs1}(2900)^0$ . Therefore, in the MCFTM, the state  $T_{cs1}(2900)^0$  should not be an isospin triplet if it is a compact state  $[cs][\bar{u}\ \bar{d}]$ .

# C. $[cu][\bar{s}\bar{d}]$ spectrum and $T_{c\bar{s}}^a(2900)$

Assuming the states  $T^a_{c\bar{s}}(2900)^0$  and  $T^a_{c\bar{s}}(2900)^{++}$  belong to the same isospin triplet, we also investigate the properties of the ground and P-wave states  $[cu][\bar{s}\,\bar{d}]$  with various spin, U spin, and color combinations in the MCFTM. Similar to the isospin of the antidiquark  $[\bar{u}\,\bar{d}]$  in the state  $[cs][\bar{u}\,\bar{d}]$ , we consider the U spin of the antidiquark  $[\bar{s}\,\bar{d}]$  in the state  $[cu][\bar{s}\,\bar{d}]$ . In this way, we can define U=0 for the U-spin antisymmetric  $[\bar{s}\,\bar{d}]$  and U=1 for the U-spin symmetric  $[\bar{s}\,\bar{d}]$ . In the same way, we can also define the V spin for the state  $[cd][\bar{s}\,\bar{u}]$ . Numerical results for the states

TABLE IV. Mass of the state  $[cu][\bar{s}\ \bar{d}]$  and contribution from each part of the Hamiltonian unit in MeV and the average distance units in fm. U represents the U spin, U=0 and 1 denote the antisymmetrical and symmetrical  $[\bar{s}\ \bar{d}]$ , respectively. Other symbols have the same meanings as those in Table III.

$l_c$	S	$UJ^P$	Color	Mass,Ratio	$\langle E_k \rangle$	$\langle V^{\rm CON} \rangle$	$\langle V^{\rm CM} \rangle$	$\langle V^{\rm C} \rangle$	$\langle V^\eta  angle$	$\langle V^\pi \rangle$	$\langle V^K \rangle$	$\langle V^{\sigma} \rangle$	$\langle \mathbf{r}_{12}^2 \rangle^{\frac{1}{2}}$	$\langle \mathbf{r}_{34}^2 \rangle^{\frac{1}{2}}$	$\langle \mathbf{r}_{13}^2 \rangle^{\frac{1}{2}}$	$\langle \mathbf{r}_{24}^2 \rangle^{\frac{1}{2}}$	$\langle \mathbf{r}_c^2 \rangle^{\frac{1}{2}}$
	0	$00^{+}$	$ar{f 3}_c ext{-}{f 3}_c$	2710, 60%	1309	300	-206	-1132	-27	0	-148	-87	0.73	0.66	0.64	0.95	0.59
			$6_{c}\mathbf{-\bar{6}}_{c}$	2778, 40%	1162	318	-236	-1087	5	-23	13	-75	0.73	0.81	0.55	0.93	0.45
			C.C.	2583	1461	262	-422	-1213	-14	-12	-86	-94	0.67	0.68	0.55	0.86	0.48
			$ar{f 3}_c$ - $f 3}_c$	2757, 94%	1254	315	-155	-1100	-27	0	-147	-84	0.76	0.66	0.65	0.98	0.59
0	1	$01^{+}$	$6_c$ - $\mathbf{\bar{6}}_c$	3003, 6%	905	396	1	-951	2	0	9	-60	0.83	0.88	0.62	1.04	0.52
			C.C.	2737	1273	308	-186	-1112	-25	0	-137		0.75	0.67	0.63	0.96	0.57
	2	$02^{+}$	$6_c$ - $\bar{6}_c$	3073, 100%	838	422	61	<b>-</b> 909	1	7	8	<b>-</b> 56	0.85	0.91	0.65	1.07	0.54
			$\bar{3}_c$ - $3_c$	2923, 75%	978	354	-27	-993	5	-18	-18	-69	0.74	0.81	0.66	1.00	0.58
	0	$10^{+}$	$6_{c}\mathbf{-\bar{6}}_{c}$	3048, 25%	865	417	36	-929	-3	0	17	-56	0.83	0.92	0.63	1.06	0.52
			C.C.	2837	1075	331	-137	-1041	3	-15	<b>-</b> 7	-73	0.72	0.80	0.61	0.96	0.52
			$ar{f 3}_c$ - $f 3}_c$	2944, 77%	942	368	-10	<b>-</b> 978	3	0	-16	-66	0.74	0.83	0.69	1.02	0.61
0	1	$11^{+}$	$6_c$ - $\mathbf{\bar{6}}_c$	3033, 23%	879	410	21	-936	-3	0	18	-57	0.82	0.92	0.63	1.05	0.52
			C.C.	2907	987	357	-64	<b>-</b> 999	1	0	-8	-68	0.73	0.83	0.65	1.00	0.57
2	12+	$ar{f 3}_c ext{-}{f 3}_c$	3028, 100%	858	398	64	-926	2	7	-15	<b>-6</b> 1	0.79	0.85	0.71	1.07	0.63	
			$\bar{3}_c$ - $3_c$	3013, 94%	1294	405	-191	-967	-25	0	-136	-68	0.76	0.69	0.86	1.15	0.84
	0	01-	$6_{c}\mathbf{\overline{6}}_{c}$	3270, 6%	1027	469	-123	-752	2	-11	7	-50	0.83	0.93	0.79	1.16	0.70
			C.C.	2992	1316	393	-229	-970	-23	-1	-126	-69	0.75	0.70	0.86	1.13	0.81
			$ar{f 3}_c$ - $f 3}_c$	3055, 99%	1251	421	-147	-943	-25	0	-136	-67	0.80	0.69	0.89	1.17	0.85
1	1	$00^-, 01^-, 02^-$	$6_c$ - $\mathbf{\bar{6}}_c$	3393, 1%	901	524	1	-697	1	0	6	-44	0.89	0.96	0.84	1.23	0.75
			C.C.	3051	1255	418	-154	-944	-24	0	-134	-67	0.80	0.69	0.88	1.17	0.84
	2	01-, 02-, 03-	$6_c$ - $\mathbf{\bar{6}}_c$	3432, 100%	865	541	33	<b>−677</b>	1	4	6	<b>-42</b>	0.90	0.97	0.86	1.25	0.77
			$\bar{3}_c$ - $3_c$	3228, 92%	970	470	-1	-839	3	<b>-</b> 9	-15	-51	0.79	0.86	0.89	1.20	0.83
	0	11-	$6_c$ - $\mathbf{\bar{6}}_c$	3429, 8%	878	544	28	-691	-2	0	11	<b>-4</b> 1	0.90	1.00	0.85	1.25	0.76
			C.C.	3208	1001	459	-40	-843	3	<b>-</b> 9	-12	-52	0.78	0.86	0.87	1.18	0.80
			$ar{f 3}_c$ - $f 3}_c$	3231, 97%	969	474	<b>-</b> 9	-843	3	0	-14	-50	0.77	0.87	0.92	1.21	0.85
1	1	10-, 11-, 12-	$6_c$ - $\mathbf{\bar{6}}_c$	3416, 3%	887	538	17	-694	-2	0	11	<b>-42</b>	0.88	1.00	0.85	1.24	
			C.C.	3222	980	470	-23	-844	2	0		-51	0.77	0.87	0.91		0.87
	2	11-, 12-, 13-	$\bar{3}_c$ - $3_c$	3291, 100%	908	500	50	-812	2	4	-14	-48	0.81	0.87	0.94	1.25	0.87

 $[cu][\bar{s}\ \bar{d}]$  are presented in Table IV. It can be found from Tables III and IV that the states  $[cs][\bar{u}\ \bar{d}]$  and  $[cu][\bar{s}\ \bar{d}]$  have a similar spectrum.

In the low-spin  $(S \leq 1)$  states  $[cu][\bar{s} \ \bar{d}]$  and  $[cs][\bar{u} \ \bar{d}]$ , the magnitude of the  $\pi$ - and K-meson-exchange interactions is distinguished, which results in their mass difference. The masses of the states  $[cu][\bar{s} \ \bar{d}]$  with U=1 are slightly lower than those of the states  $[cs][\bar{u} \ \bar{d}]$  with I=1, which mainly originates from the different contribution from the K-meson-exchange interaction. In the states  $[cu][\bar{s} \ \bar{d}]$  with U=1, the interaction can provide a small attraction, while the interaction vanishes in the states  $[cs][\bar{u} \ \bar{d}]$ . However, the states  $[cu][\bar{s} \ \bar{d}]$  with U=0 are much higher than those of the states  $[cs][\bar{u} \ \bar{d}]$  with I=0 because of the strong attraction induced by the  $\pi$ -meson-exchange interaction. The high-spin (S=2) states  $[cu][\bar{s} \ \bar{d}]$  and  $[cs][\bar{u} \ \bar{d}]$  are almost degenerate because both the  $\pi$ - and K-meson-exchange interactions are very weak.

Using the QCD sum rules, the doubly charged states  $[sd][\bar{u}\ \bar{c}]$  with the spin-parity of  $0^+$ ,  $0^-$ , and  $1^+$  have been explored [48]. The states with  $0^+$  and  $1^+$  have masses of  $2628^{+166}_{-153}$  and  $2826^{+134}_{-157}$  MeV [48], respectively, which are consistent with the corresponding results in the present work within the error range. The mass of the state with  $0^-$  is  $2719^{+144}_{-156}$  MeV [19], which is much lower than that of the state in the present work. Using QCD sum rules, the state  $[sd][\bar{u}\ \bar{c}]$  with  $1^-$  has been investigated and gives a mass of  $3515\pm125$  MeV [48], which is much higher than the model prediction on the state.

The mass of the state  $[cu]_{\bar{\mathbf{3}}_c}[\bar{\mathbf{3}}\bar{d}]_{\mathbf{3}_c}$  with  $U(J^P)=1(0^+)$  is 2923 MeV, see Table IV, which is highly consistent with those of the states  $T^a_{c\bar{s}0}(2900)^0$  and  $T^a_{c\bar{s}0}(2900)^{++}$  reported by the LHCb Collaboration. The state is a compact state composed of an axial vector  $[cu]_{\bar{3}_c}$  and an axial vector  $[\bar{s} \bar{d}]_{\mathbf{3}_c}$ . The state  $[cu]_{\mathbf{6}_c}[\bar{s} \bar{d}]_{\mathbf{6}_c}$  with  $U(J^P)=1(0^+)$  is much higher than those of the states  $T_{c\bar{s}0}^a(2900)^0$  and  $T_{c\bar{s}0}^a(2900)^{++}$ . After coupling two color configurations, the mass of the state  $[cu][\bar{s} \bar{d}]$  with  $U(J^P) = 1(0^+)$  can be decreased to 2837 MeV, which is slightly lighter than those of the states  $T_{c\bar{s}0}^a(2900)^0$  and  $T_{c\bar{s}0}^a(2900)^{++}$ . Therefore, the state  $[cu][\bar{s}\,\bar{d}]$  with  $U(J^P)=1(0^+)$  may be the main component of the states  $T^a_{c\bar{s}0}(2900)^0$  and  $T^a_{c\bar{s}0}(2900)^{++}$ . The state  $[cu][\bar{s}\bar{d}]$  with  $U(J^P) = 0(0^+)$ , the partner of the states  $T_{c\bar{s}0}^a(2900)^0$  and  $T_{c\bar{s}0}^a(2900)^{++}$ , may exist and has a mass of about 2583 MeV in the model.

## V. SUMMARY

With the Gaussian expansion method as a high precision method, in this work we employ the multiquark color fluxtube model to perform a systematic investigation on the properties of the ground and P-wave states  $[cs][\bar{u}\ \bar{d}]$  and  $[cu][\bar{s}\ \bar{d}]$  with various spin, isospin, or U spin and color combinations in the present work. The model includes a multibody confinement potential, the one-gluon-exchange interaction, the one-boson-exchange interaction ( $\pi$ , K, and  $\eta$ ), and the  $\sigma$ -meson-exchange interaction. The multibody confinement potential is a collective degree of freedom, which can bind all particles together to establish a compact state. The states  $[cs][\bar{u}\ \bar{d}]$  and  $[cu][\bar{s}\ \bar{d}]$  have similar mass spectra in the model. The mass difference between two states mainly originates from the different magnitudes of the  $\pi$ - and K-meson-exchange interactions in the states.

Matching our results with the spin-parity and mass of the states  $T_{cs0}(2900)^0$  and  $T_{cs1}(2900)^0$  reported by the LHCb Collaboration, we can describe them as the compact states  $[cs][\bar{u}\ \bar{d}]$  with  $I(J^P)=1(0^+)$  and  $0(1^-)$  in the model, respectively. The ground state  $T_{cs0}(2900)^0$  is mainly made of strongly overlapped axial vector  $[cs]_{\bar{3}_c}$  and axial vector  $[\bar{u}\ \bar{d}]_{3_c}$ . If the state  $T_{cs0}(2900)^0$  really belongs to an isotriplet within the diquark-antidiquark picture, its charged partners would be abundant in the model. The P-wave state  $T_{cs1}(2900)^0$  dominantly consists of a gradually separated scalar or axial vector  $[cs]_{\bar{3}_c}$  and a scalar  $[\bar{u}\ \bar{d}]_{3_c}$  in the shape of a dumbbell. In addition, the states  $[cs][\bar{u}\ \bar{d}]$  with  $I(J^P)=0(0^+)$  and  $0(1^+)$  may exist and the predicted masses are about 2500–2600 MeV.

The predicted mass of the state  $[[cu]_{\bar{3}_c}[\bar{s}\ \bar{d}]_{3_c}]_{1_c}$  with  $U(J^P)=1(0^+)$  in the model is in good agreement with that of the states  $T^a_{c\bar{s}0}(2900)^0$  and  $T^a_{c\bar{s}0}(2900)^{++}$ . After considering the coupling of two color configurations, the state  $[cu][\bar{s}\ \bar{d}]$  is slightly lighter than the states  $T^a_{c\bar{s}0}(2900)^0$  and  $T^a_{c\bar{s}0}(2900)^{++}$ . In this way, we cannot exclude the possibility that the state  $[cu][\bar{s}\ \bar{d}]$  with  $U(J^P)=1(0^+)$  may be the main component of the states  $T^a_{c\bar{s}0}(2900)^0$  and  $T^a_{c\bar{s}0}(2900)^{++}$  in the model. The state  $[cu][\bar{s}\ \bar{d}]$  with  $U(J^P)=0(0^+)$ , the partner of the states  $T^a_{c\bar{s}0}(2900)^0$  and  $T^a_{c\bar{s}0}(2900)^{++}$ , may exist and has a predicted mass of about 2583 MeV.

Hopefully, the systematic investigation of the states  $[cs][\bar{u}\ \bar{d}]$  and  $[cu][\bar{s}\ \bar{d}]$  will be useful for the understanding of the properties of the exotic states  $T_{cs}(2900)$  and  $T_{c\bar{s}}^a(2900)$  and the search of the new tetraquark states. We also expect more experimental and theoretical investigations to verify and understand the tetraquark states in the future.

#### **ACKNOWLEDGMENTS**

This work is partly supported by the Chongqing Natural Science Foundation under Project No. cstc2021jcyj-msxmX0078 and Fundamental Research Funds for the Central Universities under Contract No. SWU118111.

- [1] R. Aaij *et al.* (LHCb Collaboration), Phys. Rev. Lett. **125**, 242001 (2020); Phys. Rev. D **102**, 112003 (2020).
- [2] LHCb Collaboration, arXiv:2206.15233.
- [3] https://indico.cern.ch/event/1176505/.
- [4] H. X. Chen, W. Chen, R. R. Dong, and N. Su, Chin. Phys. Lett. 37, 101201 (2020).
- [5] R. Molina and E. Oset, Phys. Lett. B 811, 135870 (2020).
- [6] M. Z. Liu, J. J. Xie, and L. S. Geng, Phys. Rev. D 102, 091502(R) (2020).
- [7] M. W. Hu, X. Y. Lao, P. Ling, and Q. Wang, Chin. Phys. C 45, 021003 (2021).
- [8] C. J. Xiao, D. Y. Chen, Y. B. Dong, and G. W. Meng, Phys. Rev. D 103, 034004 (2021).
- [9] S. S. Agaev, K. Azizi, and H. Sundu, J. Phys. G 48, 085012 (2021).
- [10] Y. Y. Xue, X. Jin, H. X. Huang, J. L. Ping, and F. Wang, Phys. Rev. D 103, 054010 (2021).
- [11] B. Wang and S. L. Zhu, Eur. Phys. J. C 82, 419 (2022).
- [12] L. R. Dai, R. Molina, and E. Oset, Phys. Lett. B 832, 137219 (2022); Phys. Rev. D 105, 096022 (2022).
- [13] J. He and D. Y. Chen, Chin. Phys. C 45, 063102 (2021).
- [14] J. J. Qi, Z. Y. Wang, Z. F. Zhang, and X. H. Guo, Eur. Phys. J. C 81, 639 (2021).
- [15] H. Chen, H. R. Qi, and H. Q. Zheng, Eur. Phys. J. C 81, 812 (2021).
- [16] S. S. Agaev, K. Azizi, and H. Sundu, arXiv:2207.02648.
- [17] R. Chen and Q. Huang, arXiv:2208.10196.
- [18] S. S. Agaev, K. Azizi, and H. Sundu, Nucl. Phys. A1011, 122202 (2021).
- [19] S. S. Agaev, K. Azizi, and H. Sundu, Phys. Lett. B 820, 136530 (2021).
- [20] U. Özdem and K. Azizi, Eur. Phys. J. A 58, 171 (2022).
- [21] M. Karliner and J. L. Rosner, Phys. Rev. D 102, 094016 (2020).
- [22] J. B. Cheng, S. Y. Li, Y. R. Liu, Y. N. Liu, Z. G. Si, and T. Yao, Phys. Rev. D 101, 114017 (2020).
- [23] J. R. Zhang, Phys. Rev. D 103, 054019 (2021).
- [24] G. J. Wang, L. Meng, L. Y. Xiao, M. Oka, and S. L. Zhu, Eur. Phys. J. C 81, 188 (2021).
- [25] Q. F. Lü, D. Y. Chen, and Y. B. Dong, Phys. Rev. D 102, 074021 (2020).

- [26] Z. G. Wang, Int. J. Mod. Phys. A 35, 2050187 (2020).
- [27] G. Yang, J. Ping, and J. Segovia, Phys. Rev. D 103, 074011 (2021).
- [28] T. Guo, J. N Li, J. X. Zhao, and L. Y. He, Phys. Rev. D 105, 054018 (2022).
- [29] R. M. Albuquerque, S. Narison, D. Rabetiarivony, and G. Randriamanatrika, Nucl. Phys. A1007, 122113 (2021).
- [30] X. H. Liu, M. J. Yan, H. W. Ke, G. Li, and J. J. Xie, Eur. Phys. J. C 80, 1178 (2020).
- [31] Y. H. Ge, X. H. Liu, and H. W. Ke, Eur. Phys. J. C **82**, 955 (2022).
- [32] T. J. Burns and E. S. Swanson, Phys. Lett. B 813, 136057 (2021).
- [33] H. X. Chen, W. Chen, X. Liu, Y. R. Liu, and S. L. Zhu, arXiv:2204.02649.
- [34] C. R. Deng, H. Chen, and J. L. Ping, Phys. Rev. D 101, 054039 (2020).
- [35] T. T. Takahashi, H. Suganuma, Y. Nemoto, and H. Matsufuru, Phys. Rev. D 65, 114509 (2002).
- [36] F. Okiharu, H. Suganuma, and T. T. Takahashi, Phys. Rev. Lett. 94, 192001 (2005).
- [37] J. Vijande, F. Fernandez, and A. Valcarce, J. Phys. G 31, 481 (2005).
- [38] G. S. Bali, Phys. Rev. D **62**, 114503 (2000).
- [39] C. Semay, Eur. Phys. J. A 22, 353 (2004).
- [40] N. Cardoso, M. Cardoso, and P. Bicudo, Phys. Lett. B 710, 343 (2012).
- [41] A. Manohar and H. Georgi, Nucl. Phys. **B234**, 189 (1984).
- [42] M. D. Scadron, Phys. Rev. D 26, 239 (1982).
- [43] E. Hiyama, Y. Kino, and M. Kamimura, Prog. Part. Nucl. Phys. 51, 223 (2003).
- [44] C. R. Deng and S. L. Zhu, Sci. Bull. 67, 1522 (2022).
- [45] F. James and M. Roos, Comput. Phys. Commun. 10, 343 (1975).
- [46] C. R. Deng, H. Chen, and J. L. Ping, Eur. Phys. J. A 56, 9 (2020).
- [47] C. R. Deng, H. Chen, and J. L. Ping, Phys. Rev. D 103, 014001 (2021).
- [48] S. S. Agaev, K. Azizi, and H. Sundu, Eur. Phys. J. C 78, 141 (2018).